Manipulating the rotational properties of a two-component Bose gas

J. Christensson[1], S. Bargi[1], K. Kärkkäinen[1], Y. Yu[1], G. M. Kavoulakis[1], M. Manninen[2], and S. M. Reimann[1]
[1]*Mathematical Physics, Lund Institute of Technology, P.O. Box 118, SE-22100 Lund, Sweden*
[2]*Nanoscience Center, Department of Physics, FIN-40014 University of Jyväskylä, Finland*
(Dated: February 1, 2008)

A rotating, two-component Bose-Einstein condensate is shown to exhibit vortices of multiple quantization, which are possible due to the interatomic interactions between the two species. Also, persistent currents are absent in this system. Finally, the order parameter has a very simple structure for a range of angular momenta.

PACS numbers: 05.30.Jp, 03.75.Lm, 67.40.-w

When a superfluid is set into rotation, it demonstrates many fascinating phenomena, such as quantized vortex states and persistent flow [1]. The studies of rotational properties of superfluids originated some decades ago, mostly in connection with liquid Helium, nuclei, and neutron stars. More recently, similar properties have also been studied extensively in cold gases of trapped atoms.

Quantum gases of atoms provide an ideal system for studying multi-component superfluids. At first sight, the rotational properties of a multi-component gas may look like a trivial generalization of the case of a single component. However, as long as the different components interact and exchange angular momentum, the extra degrees of freedom associated with the motion of each species is not at all a trivial effect. On the contrary, this coupled system may demonstrate some very different phenomena, see, e.g., Refs. [2, 3, 4]. Several experimental and theoretical studies have been performed on this problem, see, e.g., Refs. [5, 6, 7, 8, 9, 10, 11], as well as the review article of Ref. [12].

In this Letter, the rotational properties of a superfluid that consists of two distinguishable components are examined. Three new and surprising conclusions result from our study:

Firstly, under appropriate conditions, one may achieve vortex states of multiple quantization. It is important to note that these states result from the interaction between the different species, and not from the functional form of the external confinement. It is well known from older studies of single-component gases, that any external potential that increases more rapidly than quadratically gives rise to vortex states of multiple quantization, for sufficiently weak interactions [13]; on the contrary, in a harmonic potential, the vortex states are always singly-quantized. In the present study, vortex states of multiple quantization result purely because of the interaction between the different components, even in a harmonic external potential. Therefore, our study may serve as an alternative way to achieve such states [14].

Secondly, our simulations indicate that multi-component gases do not support persistent currents, in agreement with older studies of homogeneous superfluids [3]. Essentially, the energy barrier that separates the (metastable) state with circulation/flow from the non-rotating state, is absent in this case, as the numerical results, as well as the intuitive arguments presented below, suggest.

Finally, we investigate the structure of the lowest state of the gas, in the range of the total angular momentum L between zero and $N_{\rm min} = \min(N_A, N_B)$, where N_A and N_B are the populations of the two species labelled as A and B. In this range of L, only the single-particle states with $m = 0$ and $m = 1$ are macroscopically occupied, as derived in Ref. [15] within the approximation of the lowest Landau level of weak interactions. Remarkably, our numerical simulations within the mean-field approximation, which go well beyond the limit of weak interactions, show that this result is more general.

For simplicity we assume equal masses for the atoms of the two components, $M_A = M_B = M$. Also, we model the elastic collisions between the atoms by a contact potential, with equal scattering lengths for collisions between the same species and different species, $a_{AA} = a_{BB} = a_{AB} = a$ (except in Fig. 4). Our results are not sensitive to the above equality and hold even if $a_{AA} \approx a_{BB} \approx a_{AB}$, as in Rubidium, for example. For the atom populations we assume $N_A \neq N_B$, but $N_A/N_B \lesssim 1$ (without loss of generality). The trapping potential is assumed to be harmonic, $V_{\rm ext}(\mathbf{r}) = M(\omega^2\rho^2 + \omega_z^2 z^2)/2$. Our Hamiltonian is thus

$$\hat{H} = \sum_{i=1}^{N_A+N_B} -\frac{\hbar^2\nabla_i^2}{2M} + V_{\rm ext}(\mathbf{r}_i) + \frac{U_0}{2}\sum_{i\neq j=1}^{N_A+N_B}\delta(\mathbf{r}_i - \mathbf{r}_j), \quad (1)$$

where $U_0 = 4\pi\hbar^2 a/M$. We consider rotation around the z axis, and also assume that $\hbar\omega_z \gg \hbar\omega$, and $\hbar\omega_z \gg n_0 U_0$, where n_0 is the typical atom density. With these assumptions, our problem becomes effectively two-dimensional, as the atoms reside in the lowest harmonic oscillator state along the axis of rotation. Thus, there are only two quantum numbers that characterize the motion of the atoms, the number of radial nodes n, and the quantum number m associated with the angular momentum. The corresponding eigenstates of the harmonic oscillator in two dimensions are labelled as $\Phi_{n,m}$.

Within the mean-field approximation, the energy of the gas in the rest frame is

$$E = \sum_{i=A,B}\int \Psi_i^*\left(-\frac{\hbar^2\nabla^2}{2M} + V_{\rm ext}(\mathbf{r})\right)\Psi_i\, d^3r +$$

$$+ \frac{U_0}{2}\int (|\Psi_A|^4 + |\Psi_B|^4 + 2|\Psi_A|^2|\Psi_B|^2)\, d^3r, \quad (2)$$

where Ψ_A and Ψ_B are the order parameters of the two components. By considering variations in Ψ_A^* and Ψ_B^*, we get the two coupled Gross-Pitaevskii-like equations,

$$\begin{aligned}\left(-\frac{\hbar^2\nabla^2}{2M} + V_{\rm ext} + U_0|\Psi_B|^2\right)\Psi_A + U_0|\Psi_A|^2\Psi_A &= \mu_A\Psi_A,\\ \left(-\frac{\hbar^2\nabla^2}{2M} + V_{\rm ext} + U_0|\Psi_A|^2\right)\Psi_B + U_0|\Psi_B|^2\Psi_B &= \mu_B\Psi_B,\end{aligned} \quad (3)$$

where μ_A and μ_B is the chemical potential of each component. We use the method of relaxation [16] to minimize the energy of Eq. (2) in the rotating frame, $E' = E - L\Omega$, where Ω is its angular velocity.

For the diagonalization of the many-body Hamiltonian, we further assume weak interactions, $n_0U_0 \ll \hbar\omega$, and work within the subspace of the states of the lowest Landau level, with $n = 0$. This condition is not necessary, however it allows us to consider a relatively larger number of atoms and higher values of the angular momentum. We consider all the Fock states which are eigenstates of the number operators $\hat{N}_A$, $\hat{N}_B$ of each species, and of the operator of the total angular momentum $\hat{L}$, and diagonalize the resulting matrix.

Combination of the mean-field approximation and of numerical diagonalization of the many-body Hamiltonian allows us to examine both limits of weak as well as strong interactions. For obvious reasons we use the diagonalization in the limit of weak interactions, and the mean-field approximation (mostly) in the limit of strong interactions. The interaction energy is measured in units of $v_0 = U_0\int|\Phi_{0,0}(x,y)|^4|\phi_0(z)|^4\, d^3r = (2/\pi)^{1/2}\hbar\omega a/a_z$, where $\phi_0(z)$ is the lowest state of the oscillator potential along the z axis, and $a_z = (\hbar/M\omega_z)^{1/2}$ is the oscillator length along this axis. For convenience we introduce the dimensionless constant $\gamma = Nv_0/\hbar\omega = \sqrt{2/\pi}Na/a_z$, with $N = N_A + N_B$ being the total number of atoms, which measures the strength of the interaction.

We first study the limit of weak coupling, $\gamma \ll 1$, and use numerical diagonalization. Considering $N_A = 4$ and $N_B = 16$ atoms, we use the conditional probability distributions to plot the density of the two components, for $L = 4, 16, 28$, and 32, as shown in Fig. 1. When $L = 4 = N_A$, and $L = 16 = N_B$, the component whose population is equal to L forms a vortex state at the center of the trap, while the other component does not rotate, residing in the core of the vortex. This is a so-called "coreless" vortex state [5, 6, 17]. As L increases beyond $L = N_B = 16$, a second vortex enters component B, and for $L = 2N_B = 32$, this merges with the other vortex to form a doubly-quantized vortex state. For this value of $L = 32$, the smaller component A does not carry any angular momentum (apart from corrections of order $1/N$). The fact that this is indeed a doubly-quantized vortex state, is confirmed by the occupancy of the single-particle

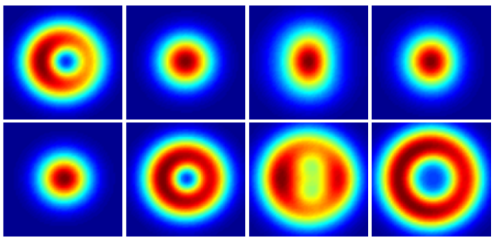

FIG. 1: The conditional probability distribution of the two components, with $N_A = 4$ (higher row), and $N_B = 16$ (lower row). Each graph extends between $-2.4a_0$ and $2.4a_0$ in both directions. The reference point is located at $(x, y) = (1.25a_0, 0)$ in the lower graphs (B component). The angular momentum L increases from left to right, $L = 4(= N_A), 16(= N_B)$, 28, and $32(= 2N_B)$.

states. By increasing N_A, N_B, and $L = 2N_B$ proportionally, we observe that the occupancy of the single-particle state with $m = 2$ of component B approaches unity, while the occupancy of all the other states are at most of order $1/N_B$. The same happens for the single-particle state with $m = 0$ of the non-rotating component A.

A similar situation emerges for the case of stronger coupling, $\gamma = 50$, where we have minimized the mean-field energy of Eq. (2) in the rotating frame (in the absence of rotation the two clouds do not phase separate). For example, we get convergent solutions, shown in Fig. 2, for $N_B/N_A = 2.777$, and (i): $L_A = N_A, L_B = 0$, for $\Omega/\omega = 0.35$ (top left), (ii) $L_A = 0, L_B = N_B$, for $\Omega/\omega = 0.45$ (top middle), (iii) $L_A = 0.755N_A, L_B = 1.171N_B$, for $\Omega/\omega = 0.555$ (top right), (iv) $L_A = 0, L_B = 2N_B$, for $\Omega/\omega = 0.60$ (bottom left), (v) $L_A = 0.876N_A, L_B = 2.057N_B$, for $\Omega/\omega = 0.69$ (bottom middle), and (vii) $L_A = 0, L_B = 3N_B$, for $\Omega/\omega = 0.73$ (bottom right). Here, L_A and L_B is the angular momentum of each component, with $L = L_A + L_B$. Again, when $L = 2N_B$, and $L = 3N_B$ the phase plots show clearly a doubly-quantized and a triply-quantized vortex state in component B, and a non-rotating cloud in component A.

The picture that appears from these calculations is intriguing: as Ω increases, a multiply-quantized vortex state of multiplicity κ splits into κ singly-quantized ones, and on the same time, one more singly-quantized vortex state enters the cloud from infinity. Eventually all these vortices merge into a multiply-quantized one of multiplicity equal to $\kappa + 1$. Figure 2 shows the above results for various values of Ω.

The mechanical stability of states which involve the gradual entry of the vortices from the periphery of the cloud is novel. This behavior is absent in one-component systems, in both harmonic, as well as anharmonic trapping potentials. In one component gases, only vortex phases of given rotational symmetry are mechanically stable [18, 19]. In the present problem, the mechanical stability of states with no rotational symmetry (shown in Fig. 2) is a consequence of the non-negative curvature of the dispersion relation (i.e., of the total energy)

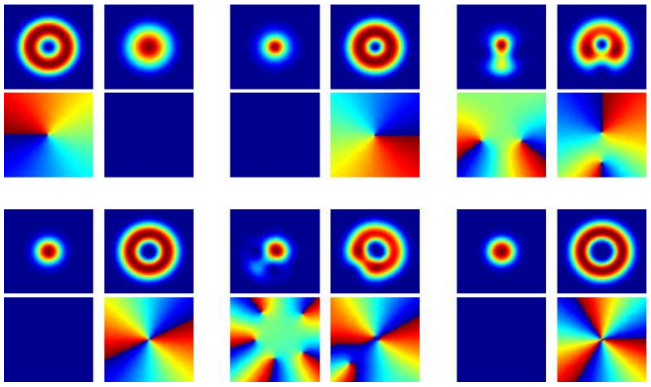

FIG. 2: The density (higher graphs of each panel) and the phase (lower graphs of each panel) of the order parameters Ψ_A (left graphs of each panel) and Ψ_B (right graphs of each panel), with $N_B/N_A = 2.777$ and a coupling $\gamma = 50$. Each graph extends between $-4.41a_0$ and $4.41a_0$ in both directions. The values of the angular momentum per atom and of Ω in each panel are given in the text.

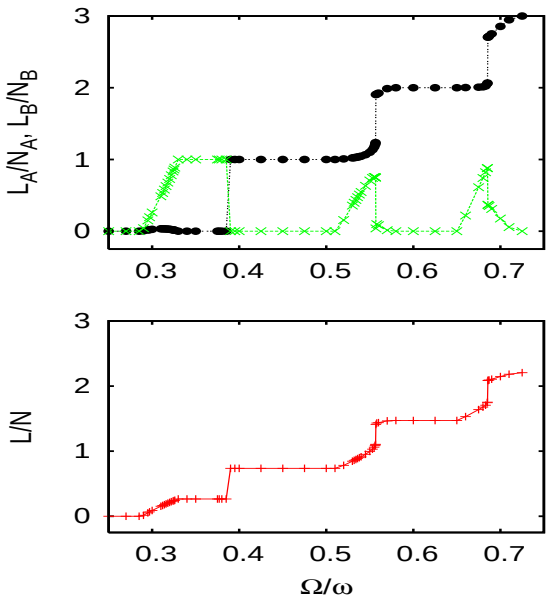

FIG. 3: Higher graph: The angular momentum L_A/N_A (crosses) and L_B/N_B (dots), as function of Ω. Lower graph: L/N as function of Ω. All curves result from the minimization of the energy in the rotating frame, within the mean-field approximation, for $\gamma = 50$.

$\mathcal{E}(L)$. This observation also connects with the (absence of) metastable, persistent currents (i.e., the second main result of our study), which we present below.

In Ref. [15] we have given a simple argument for the presence of vortex states of multiple quantization within the mean-field approximation. At least when the ratio between N_A and N_B is of order unity (but $N_A \neq N_B$), there are self-consistent solutions of Eqs. (3) of vortex states of multiple quantization. Within these solutions, the smaller component (say component A), does not rotate, providing an "effective" external potential $V_{\mathrm{eff},B}(\mathbf{r}) = V_{\mathrm{ext}}(\mathbf{r}) + U_0 n_A(\mathbf{r})$ for the other one (component B), which is anharmonic close to the center of the trap. This effectively anharmonic potential is responsible for the multiple quantization of the vortex states. Therefore, we conclude that for a relatively small population imbalance, the "coreless vortices" are vortices of multiple quantization.

The second aspect of our study is the absence of metastable currents (in the laboratory frame, for $\Omega = 0$). A convenient and physically-transparent way to think about persistent currents is that they correspond to metastable minima in the dispersion relation $\mathcal{E} = \mathcal{E}(L)$ [20]. A non-negative curvature of $\mathcal{E}(L)$ for all values of L implies the absence of metastability. For all the couplings we have examined, both within the numerical diagonalization, as well as the mean-field approximation, we have found a non-negative second derivative of the dispersion relation. Figure 3 shows L_A/N_A, L_B/N_B, and L/N versus Ω, for $\gamma = 50$. These curves are calculated by minimizing the energy $\mathcal{E}(L)$ in the rotating frame for a fixed Ω, and plotting the angular momentum per particle of the corresponding state for the given rotational frequency.

Again, our argument for the effective anharmonic potential is consistent with this positive curvature. Let us consider for simplicity $a_{AA} = a_{BB} = 0$, and $a_{AB} \neq 0$. Then, the problem of solving Eqs. (3) becomes essentially a (coupled) eigenvalue problem. If $E_{0,m}$ are the (lowest) eigenvalues of the effective (anharmonic) potential felt by the rotating component for a given angular momentum $m\hbar$, then $\partial^2 E_{0,m}/\partial m^2$ is always positive. For example, if one considers a weakly-anharmonic effective potential, $V_{\mathrm{eff}}(\rho) = M\omega^2\rho^2[1 + \lambda(\rho/a_0)^{2k}]/2$, where $k = 1, 2, \ldots$ is a positive integer, $a_0 = (\hbar/M\omega)^{1/2}$ is the oscillator length, and $0 < \lambda \ll 1$ is a small dimensionless constant, according to perturbation theory, $E_{0,m} = \hbar\omega|m| + \lambda(|m|+1)\ldots(|m|+k)/2$, which clearly has a positive curvature.

One may gain some physical insight into the absence of persistent currents by understanding the difference between a gas with one and two components. In the case of a single component, for sufficiently strong (and repulsive) interactions, an energy barrier that separates the state with circulation from the vortex-free state may develop. In the simplest model where the atoms rotate in a toroidal trap, in order for them to get rid of the circulation, they have to form a node in their density, which costs interaction energy, and this creates the energy barrier [20, 21]. On the other hand, in the presence of a second component, this node may be filled with atoms of the other species, and therefore the system may get rid of the circulation with no energy expense. This physical picture is also supported by the density plots in Figs. 2 and 4. For example, in the case of coreless vortices, the core of the vortex is filled by the other (non-rotating) component [12]. More generally, the density minima of

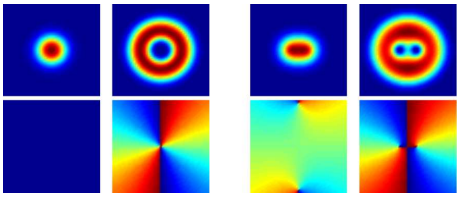

FIG. 4: The density (higher graphs) and the phase (lower graphs) of the order parameters Ψ_A (left graphs of each panel) and Ψ_B (right graphs of each panel), with $N_B/N_A = 2.777$. Here $\Omega/\omega = 0.6$ and $\gamma = 50$. In the left panel $L_A = 0$, and $L_B/N_B = 2$. In the right panel, the scattering length a_{BB} is twice as large as in the left panel, $a_{BB} = 2a$. In this case, $L_A/N_A = 0.05$, and $L_B/N_B = 1.936$. All graphs extend between $-4.41a_0$ and $4.41a_0$.

the one component coincide, roughly speaking, with the density maxima of the other component, resulting in a total density $n_{\rm tot} = |\Psi_A|^2 + |\Psi_B|^2$ which does not have any local minima or nodes.

Our third result is based on the mean-field approximation. For $0 \leq L \leq N_{\rm min}$, where $N_{\rm min} = \min(N_A, N_B)$, the only components of the order parameters Ψ_A and Ψ_B are the single-particle states with $m = 0$ and $m = 1$, i.e.,

$$\begin{aligned} \Psi_A &= \sum_n c_{n,0}\Phi_{n,0} + c_{n,1}\Phi_{n,1}, \\ \Psi_B &= \sum_n d_{n,0}\Phi_{n,0} + d_{n,1}\Phi_{n,1}, \end{aligned} \tag{4}$$

where $c_{n,0}, c_{n,1}, d_{n,0}$ and $d_{n,1}$ are functions of L and of the coupling. The numerical simulations that we perform within a range of couplings $\gamma \leq 50$ that extend well beyond the lowest-Landau level approximation, reveal this very simple structure for the lowest state of both components. Also, the corresponding dispersion relation is numerically very close to a parabola, as in the case of weak interactions [15]. Again, one may attribute these facts to the effective potential that arises from the interaction between the two species [15].

In the studies that have examined a single-component gas in an external anharmonic potential, it has been shown that as the strength of the interaction increases, there is a phase transition from the phase of multiple quantization to the phase of single quantization [19]. In the present case the situation is more complex, since the effective anharmonic potential is generated by the interaction between the two species as a result of a self-consistent solution. Still, a similar phase transition takes place here, as, for example, one keeps the scattering lengths a_{AA} and a_{AB} fixed, and increases a_{BB} that corresponds to the rotating component. Figure 4 shows the density and the phase of both species, for $a_{AA} = a_{BB} = a_{AB} = a$ (left panel), and $a_{BB} = 2a_{AA} = 2a_{AB} = 2a$ (right panel). Component B undergoes a phase transition from a doubly-quantized vortex state to two singly-quantized vortices.

To conclude, mixtures of bosons demonstrate numerous novel superfluid properties and provide a model system for studying them. Here we have given a flavor of the richness of this problem. Many of the results presented in our study are worth investigating further, as, for example, one changes the ratio of the populations, the coupling constant between the same and different species, or the masses.

We acknowledge financial support from the European Community project ULTRA-1D (NMP4-CT-2003-505457), the Swedish Research Council, the Swedish Foundation for Strategic Research, and the NordForsk Nordic Network on “Low-dimensional physics”.

[1] A. J. Leggett, Rev. Mod. Phys. **71**, S318 (1999).
[2] N. D. Mermin and T.-L. Ho, Phys. Rev. Lett. **36**, 594 (1976).
[3] P. Bhattacharyya, T.-L. Ho, and N. D. Mermin, Phys. Rev. Lett. **39**, 1290 (1977).
[4] T.-L. Ho, Phys. Rev. Lett. **49**, 1837 (1982).
[5] M. R. Matthews, B. P. Anderson, P. C. Haljan, D. S. Hall, C. E. Wieman, and E. A. Cornell, Phys. Rev. Lett. **83**, 2498 (1999).
[6] A. E. Leanhardt, Y. Shin, D. Kielpinski, D. E. Pritchard, and W. Ketterle, Phys. Rev. Lett. **90**, 140403 (2003).
[7] V. Schweikhard, I. Coddington, P. Engels, S. Tung, and E. A. Cornell, Phys. Rev. Lett. **93**, 210403 (2004).
[8] J. E. Williams and M. J. Holland, Nature (London) **401**, 568 (1999).
[9] E. J. Mueller and T.-L. Ho, Phys. Rev. Lett. **88**, 180403 (2002).
[10] K. Kasamatsu, M. Tsubota, and M. Ueda Phys. Rev. Lett. **91**, 150406 (2003).
[11] K. Kasamatsu, M. Tsubota, and M. Ueda Phys. Rev. A **71**, 043611 (2005).
[12] K. Kasamatsu, M. Tsubota, and M. Ueda, Int. J. of Mod. Phys. B, **19**, 1835 (2005).
[13] See, e.g., A. L. Fetter, Phys. Rev. A **64**, 063608 (2001); E. Lundh, Phys. Rev. A **65**, 043604 (2002), and references therein.
[14] V. Bretin, S. Stock, Y. Seurin, and J. Dalibard, Phys. Rev. Lett. **92**, 050403 (2004).
[15] S. Bargi, J. Christensson, G. M. Kavoulakis, and S. M. Reimann, Phys. Rev. Lett. **98**, 130403 (2007).
[16] See, e.g., S. A. Chin and E. Krotscheck, Phys. Rev. E **72** 036705 (2005).
[17] R. Blaauwgeers, V. B. Eltsov, M. Krusius, J. J. Ruohio, R. Schanen, and G. E.Volovik, Nature (London) **404**, 471 (2000).
[18] D. A. Butts, and D. S. Rokhsar, Nature (London) **397**, 327 (1999).
[19] See, e.g., G. M. Kavoulakis and G. Baym, New Journal of Phys. **5**, 51.1 (2003), and references therein.
[20] A. J. Leggett, Rev. Mod. Phys. **73**, 307 (2001).
[21] D. Rokhsar, e-print cond-mat/9709212.